# RAPID COMMUNICATION

## Targeting Mucosal Addressin Cellular Adhesion Molecule (MAdCAM)-1 to Noninvasively Image Experimental Crohn's Disease

CHRISTOPHER BACHMANN,*,† ALEXANDER L. KLIBANOV,§ TIMOTHY S. OLSON,‖ JASON R. SONNENSCHEIN,* JESUS RIVERA–NIEVES,* FABIO COMINELLI,* KLAUS F. LEY,†,‖ JONATHAN R. LINDNER,§ and THERESA T. PIZARRO*

*Division of Gastroenterology and Hepatology/Digestive Health Center of Excellence, †Department of Biomedical Engineering, §Division of Cardiovascular Medicine, and ‖Cardiovascular Research Center, University of Virginia Health System, Charlottesville, Virginia

*Background & Aims:* Inflammatory bowel disease (IBD) is the second most common chronic inflammatory disorder worldwide; however, a noninvasive means of accurately assessing the severity and extent of intestinal inflammation is currently not available. The aim of the present study was to develop a noninvasive imaging modality to detect and evaluate ileitis in SAMP1/YitFc (SAMP) mice. *Methods:* An image-enhancing ultrasound (US) contrast agent, consisting of encapsulated gaseous microbubbles (MB), was developed specifically to bind mucosal addressin cellular adhesion molecule-1 (MAdCAM-1), a mucosal-restricted addressin up-regulated during gut inflammation. MAdCAM-1-targeted MB ($MB_M$) were tested for binding specificity on MAdCAM-1 protein and tumor necrosis factor (TNF)-stimulated SVEC4-10 endothelial cells using an in vitro flow chamber assay and for their ability to detect and quantify ileitis by intravital microscopy and transabdominal US. *Results:* Under in vitro flow conditions, a 100-fold increase in $MB_M$ binding was observed on MAdCAM-1 protein compared with nonspecific MB ($P < .001$). TNF-stimulated endothelial cells bound significantly more $MB_M$ vs nonspecific MB ($P < .001$), which was abrogated after preincubation with anti-MAdCAM-1 antibodies ($P < .001$). In vivo, $MB_M$ specifically accumulated in focal areas of ileal inflammation and produced stronger acoustic echoes, measured by average video intensity, in SAMP vs uninflamed AKR mice ($P < .001$) or SAMP given nonspecific MB ($P < .001$). $MB_M$-specific video intensity showed a strong positive correlation with total ileal inflammatory scores ($R^2 = 0.92$). *Conclusions:* We have developed a novel intravascular US contrast agent targeting MAdCAM-1 that specifically detects and quantifies intestinal inflammation in experimental ileitis, providing the potential for a reliable, noninvasive means to diagnose and monitor disease in patients with IBD.

To date, endoscopy, barium contrast x-ray studies, computed tomography, and transabdominal ultrasound (US) are the most common procedures used by gastroenterologists to monitor patients with IBD.[1] Only endoscopy can confirm the presence of inflammation because it provides direct visual inspection of the bowel; however, it is limited to areas accessible to the endoscope and will only reveal inflammation when focal sites originating in deeper tissue layers have penetrated the lumen. The use of transabdominal US for the evaluation of Crohn's disease (CD) was implemented as early as 1979.[2] Technologic advances in high-frequency US have greatly improved resolution in recent years, and there are now several research groups actively investigating the application of transabdominal US for the management of IBD.[3–8] Visible factors, such as loss of peristalsis, increased rigidity under pressure from the US probe, wall thickness changes, and disruption of the normal 5-layer architecture have been used to assess disease severity, but it remains uncertain whether these changes are due to inflammation, fibrosis, or a combination of both.

Image-enhancing US contrast agents have been under development for a number of years and are approved by the Food and Drug Administration (FDA) for use in cardiac imaging. Recently, a more direct approach for imaging active inflammation has been made possible by conjugating antibodies to specific endothelial cell adhe-

*Abbreviations used in this paper:* DiI, indocarbocyanine; DiO, oxacarbocyanine; MAdCAM-1, mucosal addressin cellular adhesion molecule-1; MB, microbubbles; $MB_I$, isotype control microbubbles; $MB_M$, MAdCAM-1-targeted microbubbles; SAMP, SAMP1/YitFc; US, ultrasound; VI, video intensity.


0016-5085/06/$32.00
doi:10.1053/j.gastro.2005.11.009

sion molecules, expressed during an inflammatory process, to the external surface of lipid shell microbubbles (MB).[9] Of particular importance to IBD is the expression of mucosal addressin cellular adhesion molecule-1 (MAdCAM-1), a tissue-specific endothelial cell adhesion molecule that is critical for lymphocyte homing to the gut.[10] Expression of MAdCAM-1 in the adult is restricted to mucosal tissues and has been shown to be dramatically up-regulated within focal sites of intestinal inflammation in both animal models of IBD[11–17] and in human tissue samples from patients with CD and ulcerative colitis (UC).[18–20] We therefore hypothesized that development of an intravascular US contrast agent specifically targeted to MAdCAM-1 would augment existing imaging technologies and provide a means to detect and evaluate noninvasively active intestinal inflammation, such as that observed in IBD.

In the present study, targeted MB constructs were synthesized by conjugation of antibodies against MAdCAM-1 to the external surface of lipid shell MB. Specific attachment and accumulation of MAdCAM-1–specific MB ($MB_M$) was verified using an in vitro flow chamber system that has the ability to simulate a range of physiologic shear flow rates of the intestinal microcirculation across tumor necrosis factor (TNF)-stimulated cultured endothelial monolayers known to express MAdCAM-1.[21] Finally, using the SAMP1/YitFc (SAMP) mouse strain, a model of Crohn's-like ileitis that spontaneously develops chronic intestinal inflammation by 20 weeks of age with 100% penetrance,[22,23] in vivo localization of $MB_M$ was validated by intravital microscopy and contrast-enhanced transabdominal US. The severity and extent of disease in SAMP compared with uninflamed control AKR mice significantly correlated to the increased video intensity, determined by semiquantitative analysis, of the resulting US images. Therefore, we report herein the development of a novel intravascular US contrast agent specifically targeting MAdCAM-1 that can be effectively used to augment existing US-imaging technologies and that has the ability to detect and evaluate the severity of intestinal inflammation in vivo in an animal model of Crohn's ileitis. Furthermore, the targeted imaging strategy presented here lays the foundation to pursue similar technologies that have the potential to provide a cost-effective, noninvasive means to improve the diagnosis, clinical care, and management of patients with IBD.

## Materials and Methods

### Reagents

**Antibodies.** The HB-9478 (ATCC, Manassas, VA) and KLH/G2a-1-1 (Southern Biotechnology Associates, Birmingham, AL) clones were propagated to produce MECA-367 (antimurine MAdCAM-1) and isotype control rat IgG2a antibodies, respectively.clones were propagated to produce MECA-367 (antimurine MAdCAM-1) and isotype control rat IgG2a antibodies, respectively.

**Preparation of targeted MB.** Lipid shell MB were prepared by sonic dispersion of decafluorobutane gas in an aqueous medium containing phosphatidyl choline, polyethylene glycol (PEG) stearate, and biotin-PEG-distearoyl phosphatidylethanolamine (DSPE) as described previously.[24] The dialkylcarbocyanines, indocarbocyanine (DiI), or oxacarbocyanine (DiO) were incorporated into MB lipid shells for fluorescent detection and to distinguish simultaneously the $MB_M$ and isotype control MB ($MB_I$), respectively, as previously described.[24] Quantitation of biotinylated MB was determined (Coulter Multisizer IIe; Beckman Coulter, Hialeah, FL) and streptavidin (3 $\mu g/10^7$ MB) (Sigma Chemical Co., St. Louis, MO) added for 30 minutes at 0°C. Biotinylated MECA-367 or isotype control antibody was subsequently added (7.5 $\mu g$ $Ab/10^7$ MB) for 30 minutes at 0°C. Antibody-coupled MB were used immediately or aliquoted, flash frozen in liquid nitrogen, and stored at −80°C until further use.

### In Vitro Studies

**Flow cytometry.** Attachment of rat IgG2a anti-mouse MECA-367 antibodies to the external surface of lipid-shelled MB was confirmed by flow cytometry (see Figure 1*A*), following addition of Cy3-conjugated mouse anti-rat IgG antibodies (Jackson Immuno Research Laboratories, West Grove, PA). Samples were evaluated with a FACSCaliber flow cytometer (Becton-Dickinson, Franklin Lakes, NJ), which demonstrated that addition of increasing concentrations of biotinylated MECA-367 (0.0, 0.075, 0.75, 7.5, 75, 750 $\mu g$ $Ab/10^7$ MB) resulted in increased incremental fluorescence intensity until saturation was reached near 7.5 $\mu g$ $Ab/10^7$ MB. All $MB_M$ preparations used in subsequent experiments were synthesized using this concentration.

**Cell culture.** The SVEC4-10 murine endothelial cell line (ATCC) was chosen for its ability to express MAdCAM-1 following TNF stimulation.[21,25] Thirty-five-millimeter culture dishes (Corning, Corning, NY) were precoated with 5 $\mu g/cm^2$ fibronectin (Roche, Indianapolis, IN) for 2 hours at room temperature. Cells were grown to confluency using high-glucose Dulbecco's modified Eagle medium supplemented with 10% heat inactivated fetal bovine serum (FBS) and 1% penicillin-streptomycin (all from Gibco, Grand Island, NY), in 10% $CO_2$ atmosphere at 37°C and 98% humidity. Cells were cultured in the presence or absence of 20 ng/mL recombinant murine TNF (R&D Systems, Minneapolis, MN) for 24 hours and subsequently subjected to in vitro flow chamber assays.

**Flow chamber binding assay.** A commercially available Parallel Plate Flow Chamber (Glycotech, Rockville, MA) was used to modulate shear flow across recombinant MAdCAM-1 (rMAdCAM-1) substrate or cultured endothelial monolayers. A syringe pump (Harvard Appara-

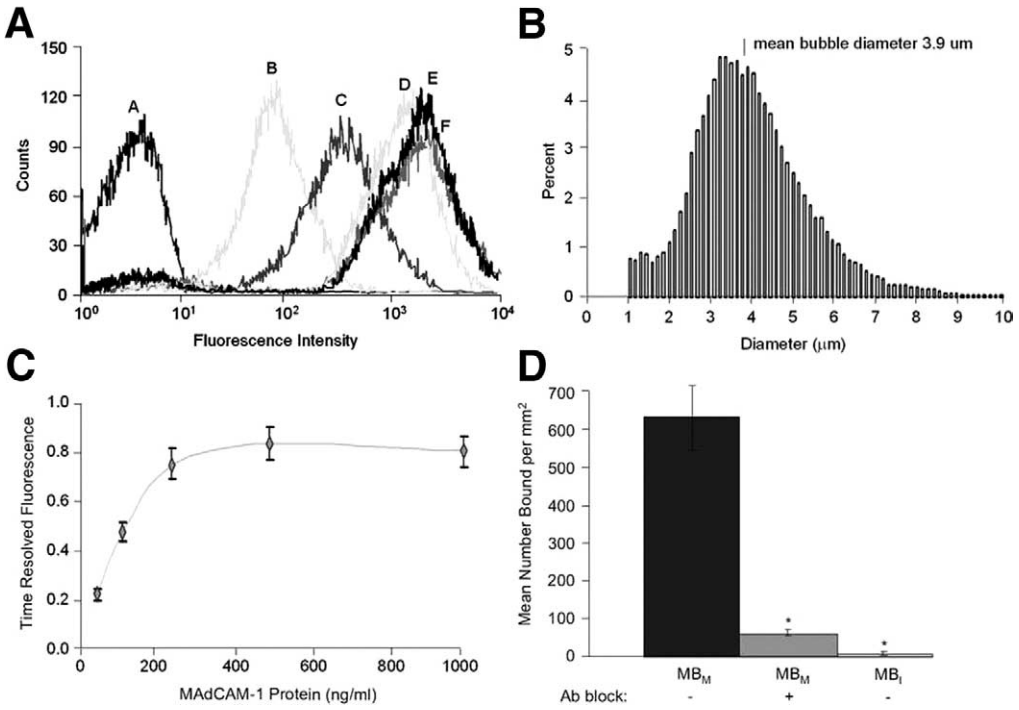


**Figure 1.** Functional evaluation of $MB_M$ constructs. (*A*) Addition of increasing concentrations of MECA-367 to bare MB (*peak A*) yielded an incremental increase in fluorescence intensity of $MB_M$ that reached saturation at ~7.5 μg Ab/$10^7$ MB (*peaks D–F*), with (*B*) a mean MB diameter of 3.9 μm following antibody conjugation. (*C*) Saturating protein concentrations of rMAdCAM-1 substrates used for in vitro flow chamber assays were determined to be 250 ng/mL, wherein (*D*) a 100-fold increase in bound $MB_M$/$mm^2$ was observed relative to control $MB_I$, and application of a blocking antibody prior to infusion of $MB_M$ significantly abrogated binding, $*P < .001$ vs $MB_M$.

tus, Holliston, MA) was used to maintain a continuous shear stress of 0.5 dyne/$cm^2$, and MB were infused at a concentration of $5 \times 10^5$ MB/mL. Twenty optical fields were recorded onto an sVHS cassette through the use of a CCD camera (Matsushita Electric Industrial Co., Ltd, Secaucus, NJ). Fluorescent excitation of DiI was used to verify the presence of bound MB.

## In Vivo Studies

**SAMP model of spontaneous ileitis.** SAMP and control AKR/J (AKR, parental background strain) mouse colonies were maintained under specific pathogen-free conditions in a barrier facility, and all in vivo experimental protocols described below were approved by the Animal Care and Use Committee at the University of Virginia. SAMP mice develop spontaneous ileitis with 100% penetrance by 20 weeks of age, with progression of disease severity over time.[22,23] SAMP and AKR mice utilized for all experiments were ≥20 weeks of age.

**Immunohistochemistry.** Mice were killed 15 minutes after MECA-367 or isotype control antibody administration (50 μg, intraperitoneally [IP]), and ileal tissues were removed, embedded in OCT (Sakura Finetek, Torrance, CA), and frozen in liquid nitrogen. Frozen tissues were then sectioned (10 μm), incubated with biotinylated secondary antibody (anti-rat IgG, Vector Laboratories, Burlingame, CA), and incubated with an avidin/biotin complex; immunoreactive cells were visualized by addition of diaminobenzidine (DAB) substrate (both from VECTASTAIN Elite ABC kit, Vector Laboratories) and counterstained in hematoxylin.

**Intravital microscopy.** Mice were anesthetized with a solution (12.5 μL/g, IP) containing ketamine hydrochloride (10 mg/mL), xylazine (1 mg/mL), and atropine (0.02 mg/mL). A small segment of bowel was exteriorized through an incision made along the linea alba, and Peyer's patches were identified by visual inspection and aligned on the optical pedestal of a custom-crafted plexiglass microscope stage. Ileal preparations were viewed under fluorescence microscopy (Carl Zeiss Inc., New York, NY), and optical filters (Carl Zeiss Inc.) were used to distinguish between DiI-labeled $MB_M$ and DiO-labeled $MB_I$ that were simultaneously administered via jugular vein cannulation ($5 \times 10^6$ of each MB in 200 μL phosphate-buffered saline [PBS]).

**In vivo targeted US imaging.** Mice were anesthetized as described above. MB ($5 \times 10^6$ in 200 μL PBS) were delivered by jugular vein cannulation and mice imaged with an ATL HDI5000cv US machine (Philips Medical Systems, Best, The Netherlands) using an L7-4 transducer operating in pulse inversion mode with a mechanical index of 0.8. A pulsing interval of 10 seconds was then used to obtain the background signal from freely circulating MB. Tissue samples from regions of interest were obtained by US-guided placement of a 23-gauge needle inserted into the abdominal cavity. Mice were killed and ileal tissues harvested for histologic evaluation by a gastrointestinal (GI) pathologist blinded to the specimens, using an established scoring system and reported as total inflammatory score, as previously described.[23] All captured US images were recorded on sVHS (Matsushita Electric Industrial Co.) and transferred to digital format (Adobe Premier, Adobe Systems Incorporated, San Jose, CA) for off-line processing and analysis. Video intensity (VI) was calculated from US images with an in-house computer algorithm that subtracts a 4-frame average circulating background signal

from the initial contrast-enhanced frame and color codes the image according to gray-scale VI, as previously described.[9]

### Statistical Analysis

Significance levels for comparisons were obtained through the use of a 1-tailed Student *t* test for samples with unequal variance.

## Results

### Functional Evaluation of MAdCAM-1-Targeted Image Enhancing US Contrast Agents

The average mean MB diameter following antibody conjugation was shown to be 3.9 μm (approximate size of a red blood cell), implying that the synthesized $MB_M$ construct was small enough to navigate through the pulmonary and renal circulations en route to its target protein. To test the specificity of $MB_M$ for MAdCAM-1, a saturating protein concentration of rMAdCAM-1 substrate was established using biotinylated MECA-367 and Europeum-labeled streptavidin. Increasing plated protein concentrations resulted in incremental increases in Europeum emission until a saturation concentration of just over 250 ng/mL was reached (Figure 1*C*). Under flow conditions of 0.5 dyne/cm$^2$ (lower limits of shear rates found in the intestinal microcirculation), interaction of $MB_M$ with rMAdCAM-1 substrate resulted in a 100-fold increase in the number of bound $MB_M$/mm$^2$ relative to $MB_I$ ($P < .001$), and application of a blocking antibody against MAdCAM-1 significantly abrogated this binding ($P < .001$) (Figure 1*D*).

### $MB_M$ Specificity and Binding Are Increased on Cultured Endothelial Cells Expressing MAdCAM-1 Under In Vitro Flow Conditions

Surface expression of MAdCAM-1 on cultured SVEC4-10 endothelial monolayers was confirmed by immunocytochemistry. Unstimulated cells showed minimal constitutive expression of MAdCAM-1 (Figure 2*A*), which dramatically increased following TNF stimulation (20 ng/mL, 24 hours); staining using an isotype control antibody resulted in minimal immunoreactivity on TNF-stimulated cells (Figure 2*C*). To test the specificity of $MB_M$ binding on MAdCAM-1 expressing endothelial cells, we performed an in vitro flow chamber functional binding assay on TNF-stimulated SVEC4-10 cells. Minimum binding was observed following infusion of DiI labeled $MB_M$ across unstimulated endothelial cells (Figure 2*D* and 2*E*), whereas binding was greatly enhanced

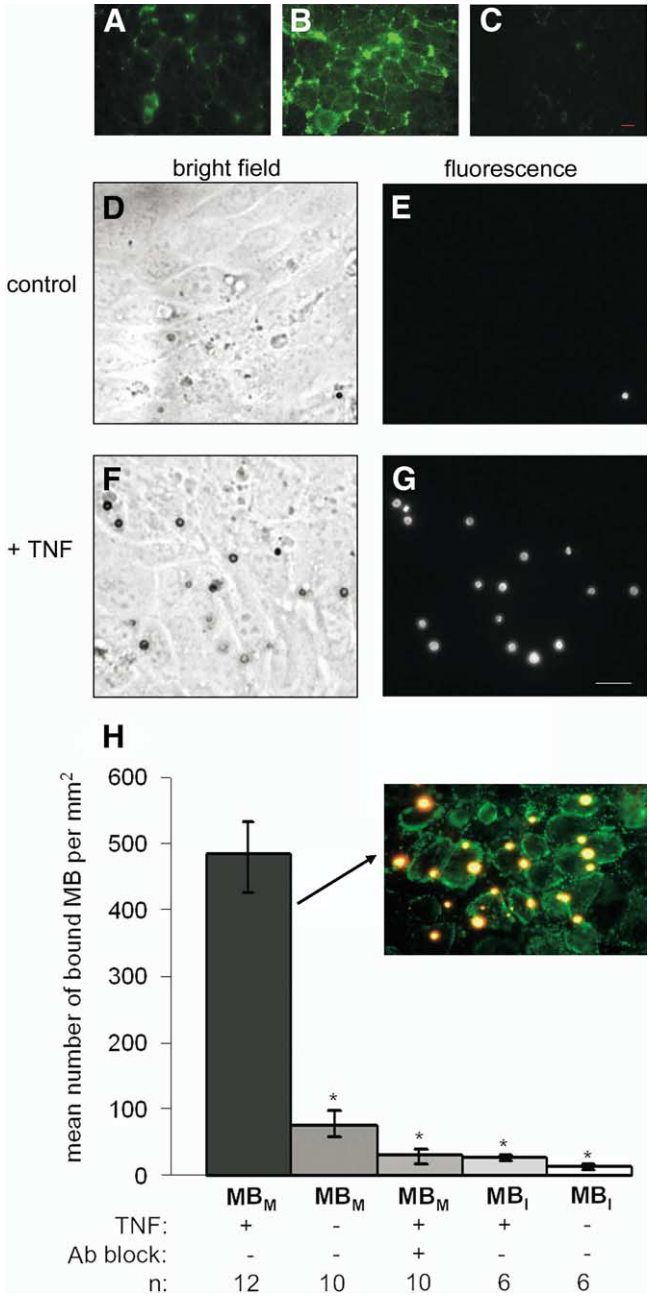


**Figure 2.** Bound $MB_M$ is increased on cultured endothelial cells expressing MAdCAM-1. (*A*) Immunocytochemistry and (*D*) representative fluorescent images of unstimulated SVEC4-10 cells showed minimal constitutive MAdCAM-1 expression and $MB_M$ binding, respectively, which dramatically increased following TNF stimulation (*B* and *E*). (*C*) Isotype control antibody on stimulated cells and (*F* and *G*) representative bright-field images of cultured SVEC4-10 cells. (*H*) Quantitative evaluation under continuous flow conditions demonstrated specificity for $MB_M$ (*inset*, labeled with *DiI*) for TNF-stimulated endothelial cells expressing MAdCAM-1 (*inset*, localized by the anti-MAdCAM-1 antibody, MECA-89, and visualized by a FITC-labeled secondary antibody) because application of anti-MAdCAM-1 blocking antibodies prior to MB infusion abrogated $MB_M$ binding and bound $MB_I$ was significantly decreased (*$P < .001$ vs $MB_M$ on TNF-stimulated cells). Results are presented as mean ± SEM; *scale bar* = 10 μm.

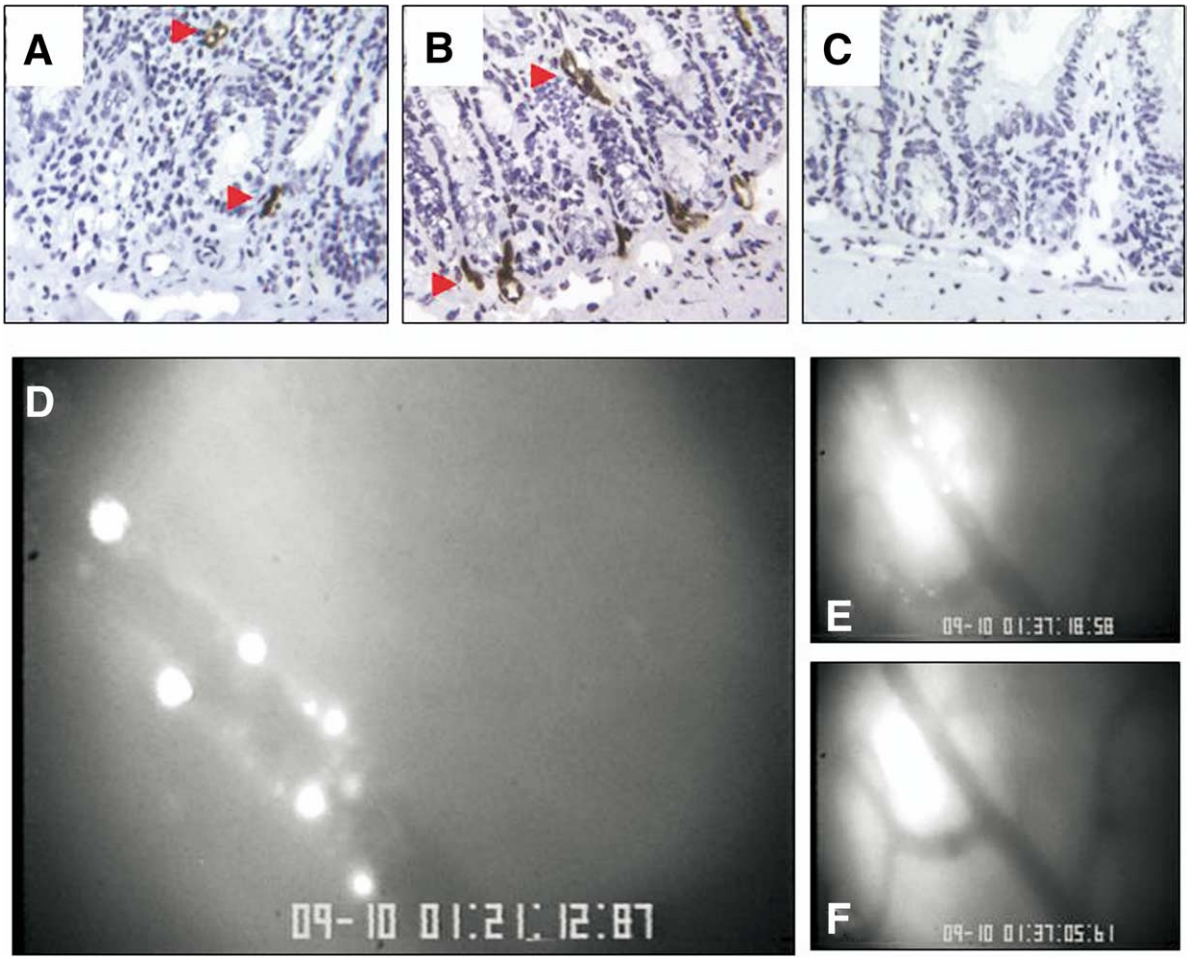


**Figure 3.** Increased MAdCAM-1 expression in SAMP ileum facilitates $MB_M$-specific binding. (*A*) Immunoreactivity for MAdCAM-1 showed basal expression on uninflamed ileum from AKR controls, which was greatly increased and immunolocalized to the microvasculature of structures morphologically consistent with lamina propria venules of SAMP mice within focal sites of ileal inflammation (*B*); (*C*) Isotype control antibodies showed no reactivity in the inflamed ileum of SAMP mice. (*D* and *E*) Intravital microscopy demonstrated $MB_M$ binding to the vascular endothelium of SAMP mice and confirmed the specificity of DiI-labeled $MB_M$ binding to vessels expressing MAdCAM-1 in SAMP ileum following simultaneous injection of $MB_M$ and $MB_I$, whereas (*F*) DiO-labeled $MB_I$ did not bind to the endothelium of the same vessels. Original magnification, panels A–C, ×20.

after stimulation with TNF (Figure 2*G*). These differences, although not apparent under bright-field microscopy, were clearly evident under fluorescence microscopy (Figure 2*D–G*). Quantitative analysis of the specific attachment and accumulation of infused $MB_M$ on cultured endothelial cells is summarized in Figure 2*H*. TNF-stimulated SVEC4-10 cells bound significantly more $MB_M$ (Figure 2*H*, inset) compared with unstimulated cells, whereas preincubation of a blocking anti-MAdCAM-1 antibody prior to infusion significantly reduced the number of adherent $MB_M$ ($484 \pm 50$ vs $75 \pm 19$ and $29 \pm 8$ $MB_M/mm^2$, respectively; $P < .001$). $MB_M$ specificity was further supported because nonspecific $MB_I$ binding was significantly reduced on both unstimulated and TNF-stimulated SVEC4-10 cells ($26 \pm 3$ and $11 \pm 2$ $MB_I/mm^2$, respectively; $P < .001$ vs $MB_M$ binding on stimulated cells).

### $MB_M$ Contrast-Enhanced Transabdominal US Detects and Correlates With the Severity of Ileal Inflammation in SAMP Mice

Immunohistochemical analysis of healthy AKR control mice showed faint basal expression of MAdCAM-1 in the terminal ileum (Figure 3*A*), whereas age-matched diseased SAMP (≥20 weeks) showed strong immunoreactivity for MAdCAM-1 on vessels morphologically consistent with venules of the lamina propria within focal areas of inflammation (Figure 3*B*). Isotype control antibodies showed no reactivity and confirmed specificity of MAdCAM-1 expression and up-regulation in the inflamed ileum of SAMP mice (Figure 3*C*). In addition, a second anti-MAdCAM-1 antibody (MECA-89) provided identical immunolocalization of MAd-

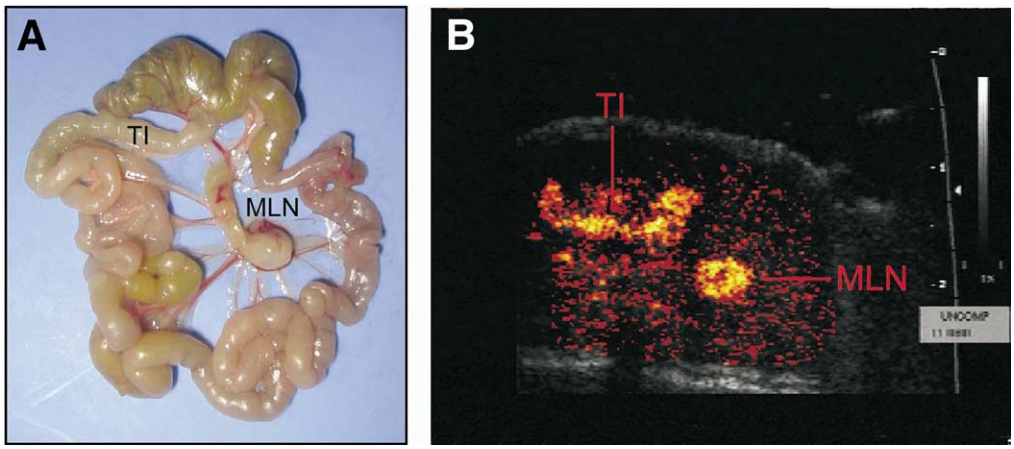


**Figure 4.** Localization and identification of inflammatory foci by $MB_M$-targeted, contrast-enhanced transabdominal US. (*A*) The inflamed terminal ileum (TI) and enlarged draining mesenteric lymph node (MLN), characteristic of SAMP mice, were identified by US-guided placement of 23-gauge needles inserted into the abdominal cavity and localized to areas clearly visible in contrast-enhanced color-coded images following $MB_M$ infusion (*B*).

CAM-1, which was abrogated following preincubation with murine rMAdCAM-1 protein (data not shown). To validate specificity of $MB_M$ on MAdCAM-1 expressing endothelial cells, intravital microscopy on preparations of SAMP Peyer's patches was performed to observe directly in vivo MB-endothelial cell interactions. $MB_M$ and $MB_I$ were fluorescently labeled with DiI and DiO, respectively, with peak emission spectrums centered around 565 and 500 nm, respectively. Following simultaneous infusion of $MB_M$ and $MB_I$ ($5 \times 10^6$ of each MB), optical filters distinguishing DiI-labeled $MB_M$ and DiO-labeled $MB_I$ showed increased accumulations of $MB_M$ throughout the microvasculature, whereas $MB_I$ showed little to no adherence on the same microvasculature (Figure 3*D* and 3*E*).

Transabdominal US was then performed on experimental mice (≥20 weeks of age) following intravascular delivery of MB constructs. US-guided placement of 23-gauge needles inserted into the abdominal cavity and aimed at strong acoustic echoes, appearing as bright regions during US imaging, corresponded to areas of macroscopically involved small intestine as well as enlarged, draining mesenteric lymph nodes upon necropsy of SAMP mice receiving $MB_M$ (Figure 4). When comparing uninflamed control mice to diseased SAMP, healthy AKR mice generated weak background signals

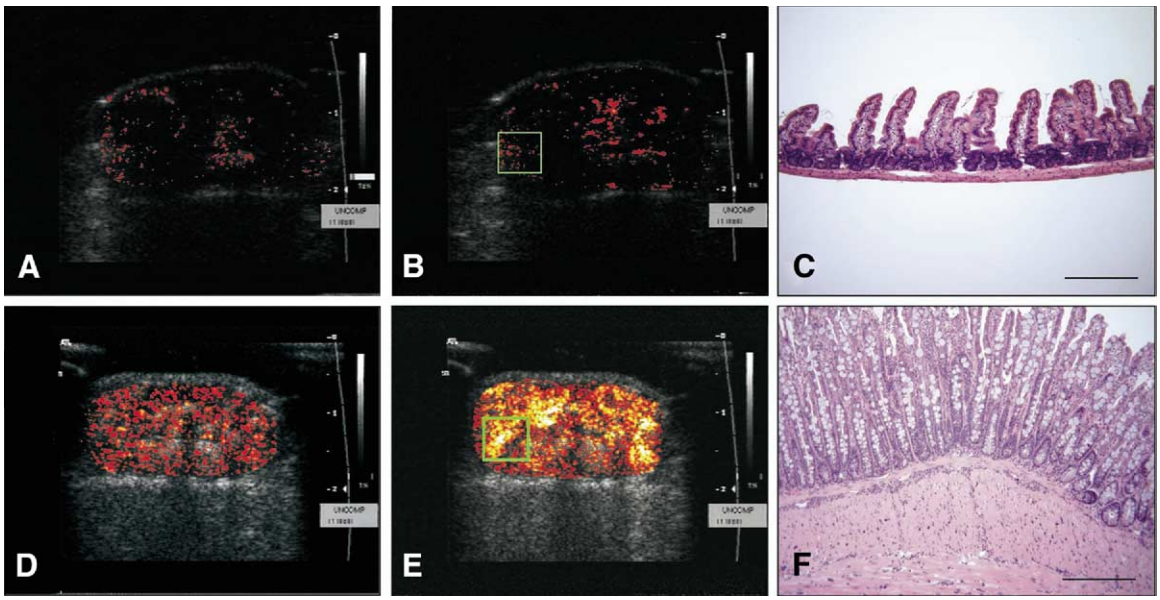


**Figure 5.** $MB_M$-targeted, contrast-enhanced transabdominal US in SAMP mice. (*A*) Healthy AKR mice showed weak background signal following either $MB_I$ or (*B*) $MB_M$ infusion, whereas (*E*) accumulations of $MB_M$ produced strong acoustic echoes that appear as *bright regions* in color-coded images. (*D*) Background subtracted color-coded images of $MB_I$ in SAMP mice produced little baseline signal. (*C*) Histologic analysis of ileal tissues isolated from AKR control (*panel B*, *green box*) showed normal bowel architecture with no evidence of inflammation, whereas (*F*) ileal tissues obtained from *bright regions* of SAMP mice showed gross morphologic changes, including acute and chronic inflammation (scale bar = 250 mm), indicative of severe disease (*scale bar* = 250 μm).

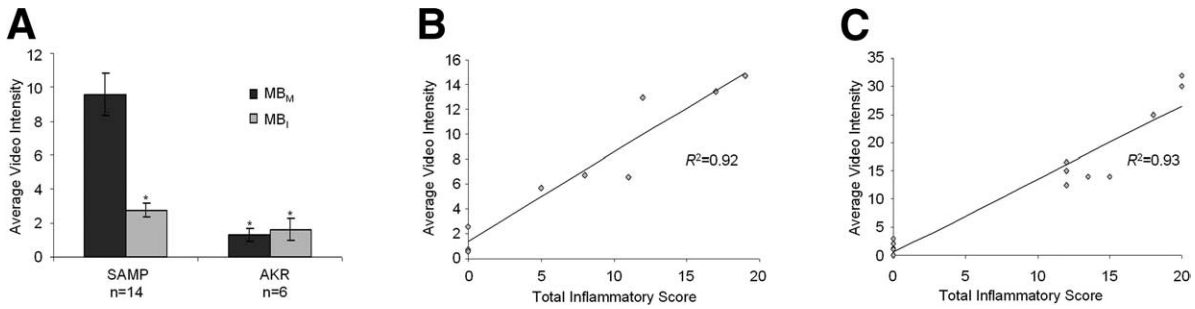


**Figure 6.** VI of $MB_M$-targeted, contrast-enhanced transabdominal US images correlated with ileal disease severity. (*A*) Diseased SAMP consistently showed a higher average VI following $MB_M$ infusion, which was significantly decreased in healthy AKR control mice and following $MB_I$ infusion (*$P < .001$ vs $MB_M$ infused SAMP); results presented as mean ± SEM. (*B*) Average VI of in vivo, as well as (*C*) ex vivo images obtained following administration of $MB_M$, showed a strong positive correlation ($R^2 = 0.92$ and 0.93, respectively) with disease severity in SAMP mice, as assessed by total inflammatory scores obtained by histologic evaluation.

following either $MB_I$ or $MB_M$ infusion (Figure 5*A* and 5*B*). Conversely, in SAMP mice, accumulations of $MB_M$ produced strong acoustic echoes, demonstrated in color-coded US images (Figure 5*E*), compared with $MB_I$ that produced little baseline signal (Figure 5*D*). In addition, small intestinal tissues obtained under US-guided placement of 23-gauge needles (Figure 5*B* and 5*E*, green box) localized to areas of inflamed ileal segments in SAMP mice showing severe villous blunting and infiltration of acute and chronic inflammatory cells (Figure 5*F*), whereas corresponding areas in AKR mice showed morphologically normal intestine with no inflammation, as determined by histologic evaluation. To quantify the signal strength of acoustic echoes received by the US transducer, background subtracted color-coded images were analyzed, and it was determined that VI of images obtained from SAMP mice infused with $MB_M$ were, on average, 900% stronger than images obtained from AKR control mice ($P < .001$); $MB_M$ consistently produced stronger acoustic echoes (increased VI) than $MB_I$ in SAMP mice ($P < .001$), whereas normal AKR mice showed weak acoustic signal strength and no significant difference in VI with either $MB_M$ or $MB_I$ (Figure 6*A*). Finally, VI of $MB_M$ contrast-enhanced in vivo and ex vivo US images showed a strong positive correlation ($R^2 = 0.92$ and 0.93, respectively) with the severity of ileitis, evaluated as total inflammatory scores, in SAMP mice (Figure 6*B* and 6*C*).

## Discussion

The use of transabdominal US for the evaluation of CD was implemented as early as 1979 wherein wall thickening of the terminal ileum and cecum, with accompanying inflammatory changes in the mesentery, yielded recognizable patterns in both longitudinal and transverse images.[2] These initial US images lacked sufficient resolution to provide a sensitive measure of disease activity, but technologic advances in high-frequency US have greatly improved resolution over the past 20 years, and there is now renewed interest in the application of US for the management of IBD. However, the use of wall thickness measurements to evaluate active intestinal inflammation, although reportedly successful in most investigations, remains a controversial issue. From the 440 patients examined by Limberg and Osswald, mean wall thickness of normal bowel was established to be 3.0 ± 0.7 mm.[4] This is consistent with the results reported by Hata et al, who established the mean overall wall thickness in normal patients to be 2.8 mm, with no normal specimens exceeding 4.0 mm.[26] These results imply that a significant portion of normal individuals would be classified as abnormal, or regions of mild to moderate inflammation would go undetected, if a strict demarcation between diseased and normal bowel is based purely on wall thickness measurements. The targeted US contrast agent developed in this study would resolve these discrepancies and render transabdominal US a powerful diagnostic tool for the management of patients with both UC and CD.

The concept of using gaseous particles to enhance US imaging was first introduced in 1968,[27] and 16 years after these initial studies, a technique for producing encapsulated MB with sizes on the order of red blood cells was produced.[28] The first generation of stable albumin-shelled MB was developed at the University of Virginia in 1987,[29] and injections in which the mean MB size was less than 6 μm successfully opacified the left ventricle in 82% of the studies, providing proof of the first peripherally injected US contrast agent durable enough to survive passage through the heart and small enough to traverse the pulmonary capillary network.[30] Subsequently, a human albumin MB encapsulating a uniquely fluorinated gas that has a low solubility in both blood and water was developed by Molecular Biosystems

(San Diego, CA) and marketed under the trade name Optison. The octafluoropropane formulation extends the temporal window of the contrast agent to more than 5 minutes, allowing enough time to traverse the entire peripheral circulation. Optison received approval by the FDA for marketing in the United States on January 5, 1998, and from the European Commission in May of that year.

Over the past several years, members of our research group have been actively developing US contrast agents similar to Optison that are specific for inflammation. Contrast-enhanced renal US images of mice undergoing ischemia-reperfusion injury have shown that a more direct method of imaging active inflammation was possible by conjugating ligands to specific endothelial cell adhesion molecules to the external surface of the lipid-shell MB.[9] In the present study, we successfully conjugated rat anti-mouse antibodies detecting MAdCAM-1 to the external surface of lipid-shelled MB to produce a targeted contrast agent for use with transabdominal US to detect experimental ileitis. The mean MB diameter following antibody conjugation was shown to be 3.9 μm (the approximate size of a red blood cell), implying that the targeted $MB_M$ construct was small enough to navigate through the pulmonary and renal circulations en route to its target protein. The present imaging strategy can be used as a research tool to further our current understanding into the pathogenesis and progression of IBD by monitoring in vivo mucosal inflammation in whole animals with colitis.

In addition, transabdominal US images obtained in the present study were acquired 5 minutes following injection of the targeted MB constructs. Postprocessing was made simple by a computational algorithm that automatically subtracted background signal from freely circulating MB to produce rapidly the color-coded images with a quantifiable measure of signal intensity. In practice, physicians could obtain a background-subtracted color-coded image of the bowel, complete with a digital measure of signal intensity, within a half hour and could do so repeatedly without imposing any significant health risk or undue discomfort on the patient.

In summary, with the current observation of a dramatic increase in the number of newly diagnosed cases of IBD in nearly all parts of the world, there exists a strong demand for a simple, inexpensive, and noninvasive procedure that will enable the gastroenterologist to assess routinely the degree and extent of active intestinal inflammation in patients with IBD. Here, we provide strong evidence that this can be potentially accomplished through the use of tissue-specific contrast imaging that extends the capabilities of existing US technologies by exploiting the natural mechanisms employed by lymphocytes for organ-specific migration.

## References


1. Kirsner JB. Inflammatory bowel disease. Philadelphia: W. B. Saunders Co, 2000.
2. Holt S, Samuel E. Grey scale ultrasound in Crohn's disease. Gut 1979;20:590–595.
3. Schwerk WB, Beckh K, Raith M. A prospective evaluation of high-resolution sonography in the diagnosis of inflammatory bowel disease. Eur J Gastroenterol Hepatol 1992;4:173–182.
4. Limberg B, Osswald B. Diagnosis and differential diagnosis of ulcerative colitis and Crohn's disease by hydrocolonic sonography. Am J Gastroenterol 1994;89:1051–1057.
5. Solvig J, Ekberg O, Lindgren S, Floren CH, Nilsson P. Ultrasound examination of the small bowel: comparison with enterolysis in patients with Crohn's disease. Abdom Imaging 1995;20:323–326.
6. Maconi G, Parente F, Bollani S, Cesana B, Bianchi Porro G. Abdominal ultrasound in the assessment of extent and activity of Crohn's disease: clinical significance and implication of bowel wall thickening. Am J Gastroenterol 1996;91:1604–1609.
7. Andreoli A, Cerro P, Falasco G, Giglio LA, Prantera C. Role of ultrasonography in the diagnosis of postsurgical recurrence of Crohn's disease. Am J Gastroenterol 1998;93:1117–1121.
8. Gasche C, Moser G, Turetschek K, Schober E, Moeschl P, Oberhuber G. Transabdominal bowel sonography for the detection of intestinal complications in Crohn's disease. Gut 1999;44:112–117.
9. Lindner JR, Song J, Christiansen J, Klibanov AL, Xu F, Ley K. Ultrasound assessment of inflammation and renal tissue injury with microbubbles targeted to P-selectin. Circulation 2001;104:2107–2112.
10. Nakache M, Berg EL, Streeter PR, Butcher EC. The mucosal vascular addressin is a tissue-specific endothelial cell adhesion molecule for circulating lymphocytes. Nature 1989;337:179–181.
11. Viney JL, Jones S, Chiu HH, Lagrimas B, Renz ME, Presta LG, Jackson D, Hillan KJ, Lew S, Fong S. Mucosal addressin cell adhesion molecule-1: a structural and functional analysis demarcates the integrin binding motif. J Immunol 1996;157:2488–2497.
12. Kato S, Hokari R, Matsuzaki K, Iwai A, Kawaguchi A, Nagao S, Miyahara T, Itoh K, Ishii H, Miura S. Amelioration of murine experimental colitis by inhibition of mucosal addressin cell adhesion molecule-1. J Pharmacol Exp Ther 2000;295:183–189.
13. Connor EM, Eppihimer MJ, Morise Z, Granger DN, Grisham MB. Expression of mucosal addressin cell adhesion molecule-1 (MAdCAM-1) in acute and chronic inflammation. J Leukoc Biol 1999;65:349–355.
14. Kawachi S, Jennings S, Panes J, Cockrell A, Laroux FS, Gray L, Perry M, van der Heyde H, Balish E, Granger DN, Specian RA, Grisham MB. Cytokine and endothelial cell adhesion molecule expression in interleukin-10-deficient mice. Am J Physiol (Gastrointest Liver Physiol) 2000;278:G734–G743.
15. McDonald SA, Palmen MJ, Van Rees EP, MacDonald TT. Characterization of the mucosal cell-mediated immune response in IL-2 knockout mice before and after the onset of colitis. Immunology 1997;91:73–80.
16. Hokari R, Kato S, Matsuzaki K, Iwai A, Kawaguchi A, Nagao S, Miyahara T, Itoh K, Sekizuka E, Nagata H, Ishii H, Iizuka T, Miyasaka M, Miura S. Involvement of mucosal addressin cell adhesion molecule-1 (MAdCAM-1) in the pathogenesis of granulomatous colitis in rats. Clin Exp Immunol 2001;126:259–265.
17. Picarella D, Hurlbut P, Rottman J, Shi X, Butcher E, Ringler DJ. Monoclonal antibodies specific for β 7 integrin and mucosal

addressin cell adhesion molecule-1 (MAdCAM-1) reduce inflammation in the colon of scid mice reconstituted with CD45RBhigh CD4+ T cells. J Immunol 1997;158:2099–2106.
18. Briskin M, Winsor-Hines D, Shyjan A, Cochran N, Bloom S, Wilson J, McEvoy LM, Butcher EC, Kassam N, Mackay CR, Newman W, Ringler DJ. Human mucosal addressin cell adhesion molecule-1 is preferentially expressed in intestinal tract and associated lymphoid tissue. Am J Pathol 1997;151:97–110.
19. Souza HS, Elia CC, Spencer J, MacDonald TT. Expression of lymphocyte-endothelial receptor-ligand pairs, $\alpha 4\beta 7$/MAdCAM-1 and OX40/OX40 ligand in the colon and jejunum of patients with inflammatory bowel disease. Gut 1999;45:856–863.
20. Arihiro S, Ohtani H, Suzuki M, Murata M, Ejima C, Oki M, Kinouchi Y, Fukushima K, Sasaki I, Nakamura S, Matsumoto T, Torii A, Toda G, Nagura H. Differential expression of mucosal addressin cell adhesion molecule-1 (MAdCAM-1) in ulcerative colitis and Crohn's disease. Pathol Int 2002;52:367–374.
21. Oshima T, Pavlick KP, Laroux FS, Verma SK, Jordan P, Grisham MB, Williams L, Alexander JS. Regulation and distribution of MAdCAM-1 in endothelial cells in vitro. Am J Physiol (Cell Physiol) 2001;281:C1096–C1105.
22. Kosiewicz MM, Nast CC, Krishnan A, Rivera-Nieves J, Moskaluk CA, Matsumoto S, Kozaiwa K, Cominelli F. Th1-type responses mediate spontaneous ileitis in a novel murine model of Crohn's disease. J Clin Invest 2001;107:695–702.
23. Rivera-Nieves J, Bamias G, Vidrich A, Marini M, Pizarro TT, McDuffie MJ, Moskaluk CA, Cohn SM, Cominelli F. Emergence of perianal fistulizing disease in the SAMP1/YitFc mouse, a spontaneous model of chronic ileitis. Gastroenterology 2003;124:972–982.
24. Klibanov AL. Targeted delivery of gas-filled microspheres, contrast agents for ultrasound imaging. Adv Drug Deliv Rev 1999;37:139–157.
25. Sikorski EE, Hallmann R, Berg EL, Butcher EC. The Peyer's patch high endothelial receptor for lymphocytes, the mucosal vascular addressin, is induced on a murine endothelial cell line by tumor necrosis factor-alpha and IL-1. J Immunol 1993;151:5239–5520.
26. Hata J, Haruma K, Suenaga K. Ultrasonographic assessment of inflammatory bowel disease. Am J Gastroenterol 1992;87:443–447.
27. Gramiak R, Shah PM. Echocardiography of the aortic root. Invest Radiol 1968;3:356–366.
28. Feinstein SB, Ten Cate FJ, Zwehl W, Ong K, Maurer G, Tei C, Shah PM, Meerbaum S, Corday E. Two-dimensional contrast echocardiography. I. In vitro development and quantitative analysis of echo contrast agents. J Am Coll Cardiol 1984;3:14–20.
29. Keller MW, Feinstein SB, Watson DD. Successful left ventricular opacification following peripheral venous injection of sonicated contrast agent: an experimental evaluation. Am Heart J 1987;114:570–575.
30. Keller MW, Glasheen W, Kaul S. Albunex: a safe and effective commercially produced agent for myocardial contrast echocardiography. J Am Soc Echocardiogr 1989;2:48–52.

**Received July 18, 2005. Accepted November 2, 2005.**

**Address requests for reprints to: Theresa T. Pizarro, PhD, Box 800708, University of Virginia Health System, Charlottesville, Virginia 22908. e-mail: ttp4e@virginia.edu; fax: (434) 243-6169.**

**Supported by grants from the Crohn's and Colitis Foundation of America (Senior Research Award, to T.T.P.), Commonwealth Technology Research Fund, "Program in Mucosal Immunology" (Pilot Feasibility, to T.T.P.), and the National Institutes of Health (P01 DK57880, to F.C., T.T.P., and K.F.L.; and P30 DK56703, to F.C. and T.T.P.).**

**The authors thank Drs. Christopher Moskaluk and James Mize for histopathologic evaluation; Leslie Hancock, Matt Staples, and Muhammadreza Sachedina for technical assistance, and the Morphology/Imaging (Sharon Hoang and Greg Harp for histologic images) and Immunology (William Ross for flow cytometry expertise) Cores of the NIH-funded Silvio O. Conte Digestive Diseases Research Center at UVA.**